
Article:
Mihai, AP, Whiteside, AL, Canwell, EJ et al. (2013) Effect of substrate temperature on the magnetic properties of epitaxial sputter-grown Co/Pt. Applied Physics Letters, 103 (26). 262401. ISSN: 0003-6951

https://doi.org/10.1063/1.4856395

Effect of substrate temperature on the magnetic properties of epitaxial sputter-grown Co/Pt

A.P. Mihai[1], A.L. Whiteside[1], E.J. Canwell[1], C.H. Marrows[1], M.J. Benitez[2], D. McGrouther[2], S. McVitie[2], S. McFadzean[2] and T.A. Moore[1,a)]

[1]*School of Physics and Astronomy, University of Leeds, Leeds, LS2 9JT, U.K.*

[2]*School of Physics and Astronomy, University of Glasgow, Glasgow* G12 8QQ*, U.K.*

Epitaxial Co/Pt films have been deposited by dc-magnetron sputtering onto heated C-plane sapphire substrates. X-ray diffraction, the residual resistivity and transmission electron microscopy indicate that the Co/Pt films are highly ordered on the atomic scale. The coercive field and the perpendicular magnetic anisotropy increase as the substrate temperature is increased from 100-250°C during deposition of the Co/Pt. Measurement of the domain wall creep velocity as a function of applied magnetic field yields the domain wall pinning energy, which scales with the coercive field. Evidence for an enhanced creep velocity in highly ordered epitaxial Co/Pt is found.

Co/Pt multilayers have been studied for a number of years[1,2], initially because of their potential as magneto-optical recording media[3]. Their attractive properties include perpendicular magnetic anisotropy (PMA) and a large polar magneto-optic Kerr effect (MOKE) at short wavelengths[4]. More recently Co/Pt has become an interesting system for the study of the physics of domain walls (DWs)[5-8], and spin torque[9-13]. The PMA leads to the formation of narrow, nanometre-scale DWs, and the large polar Kerr effect is convenient for measuring the DW motion. However, DWs tend to pin at grain boundaries in the polycrystalline Co/Pt that is typically used in these studies[9], and this is an issue not only for investigations of the fundamental physics of DWs but also for future devices which may depend upon reliable DW motion, such as racetrack memory[14]. Epitaxial Co/Pt, in which the density of grain boundaries is minimised, could provide a solution to this problem. Ideally, however, the method of multilayer deposition should be compliant with industrial processes.

Sputtering is a convenient, cost-effective technique for thin film deposition and may be used to grow films epitaxially if a single crystal substrate is heated to an appropriate temperature. In order to obtain PMA in epitaxial Co/Pt, the films are required to grow in the (111)-orientation[15], and (111) texture was first seen in sputtered Co/Pt in 1993[16]. While there have been studies of Co/Pt superlattices[17] and Pt/Co/Pt sandwiches[18] grown by sputtering, there has been no optimisation of sputtered epitaxial Co/Pt (111) for DW devices. Here we show how the substrate temperature may be used to tune the magnetic properties of epitaxial Co/Pt grown on sapphire.

First, the growth of Pt on C-plane (0001) sapphire was optimised. A 60 nm Pt film was deposited at various substrate temperatures in the range 400-700°C. High angle X-ray scans all had a clear peak between 39.5° and 40°, indicating (111) structure (see Figure 1). The

peak was largest and the satellite peaks were best defined for a deposition temperature of 500°C indicating that at this temperature the crystal quality of the film was highest. It was also found that overnight annealing of the sapphire substrate at 700 °C improved film quality. X-ray reflectivity curves were measured from Pt films deposited both after a short preheat and after an overnight anneal. For the short preheat the substrate temperature was ramped up at a rate of 5°C/min to the target temperature and held for an hour before commencing the film deposition. For the overnight anneal the substrate temperature was ramped up at a rate of 5°C/min to 700°C where it was held for four hours before being ramped down to the target temperature at a rate of 3°C/min. The reflectivity curve for the film deposited after an overnight anneal had a larger number of well-defined interference fringes up to an angle of 6° grazing incidence. This indicated a better surface quality, probably resulting from the thermal equilibrium that was achieved between the substrate and the sputter deposition system, and from the longer period of outgassing that occurred during the overnight anneal. Fitting the reflectivity curves using the GenX code[19,20] yielded a roughness of 2.26 ±0.10 Å for the overnight anneal and 2.90 ±0.10 Å for the short preheat. The residual resistivity ratio (RRR) determined from resistance versus temperature measurements and the full width-half maximum (FWHM) determined from X-ray diffraction rocking curves showed that a substrate temperature of 450-550°C during growth yielded the best quality films – those that possessed both a large RRR (~12) and a small FWHM (22×10^{-3} °).

Subsequently, $[Co(t)/Pt(1.0nm)]_{10}$ multilayers, where t = 0.5, 1.0, 1.3 nm, were deposited on top of Pt(3.0nm) while the substrate was held at a temperature of approximately 80°C. Figure 1 shows X-ray diffraction spectra for these multilayers compared with the spectrum for a single 60 nm-thick Pt layer. As the thickness of the Co layers was increased, the (111) peak shifted to higher values of 2θ, characteristic of a decrease in the out-of-plane lattice

constant *a* of the multilayer. This can be understood in the context of the changing proportions of Co and Pt in the multilayer, with thicker layers of fcc Co with a = 3.55 Å decreasing the lattice constant from its initial (Pt) value of 3.92 Å. The addition of Co also reduced the (111) peak intensity. Thus thin Co layers are required in order to maintain crystallographic continuity. The positions of the Pt and Co/Pt X-ray diffraction peaks correspond well with those measured in previous work[2].

In order to examine the crystal structure of the Co/Pt films, we used high-angular annular dark-field (HAADF) imaging in scanning transmission electron microscopy (STEM) with an electron probe < 1 nm in diameter. The contrast in the HAADF STEM mode depends strongly on the atomic number Z, and the small Z of Co compared to that of Pt means that individual layers can be identified. In Figure 2(a) the Co layer can be clearly distinguished as three rows of atoms on a dark background, contrasting with the neighbouring Pt layers which display atomic structure on a bright background. The area profile in Figure 2(b) shows the expected number of atomic layers in each material: 11-12 in 3.0 nm Pt, 3-4 in 0.7 nm Co, and 3-4 in 1.0 nm Pt. The imaging shows that, at a growth temperature of 150°C, the crystallographic ordering in the Co/Pt is good.

The next step was to determine the substrate temperature for Co/Pt layer growth that led to suitable magnetic properties for studies of DW motion. We focused on Co/Pt multilayers with 0.5 nm-thick Co and few repeats, in order to avoid stripe domains[21] and a large coercive field. Figure 3 shows the coercive field H_c and effective perpendicular magnetic anisotropy constant K_{eff} for Pt(3.0nm)/[Co(0.5nm)/Pt(1.0nm)]$_2$, with the Co/Pt layers deposited at various substrate temperatures in the range 100-250°C. H_c, obtained from polar MOKE hysteresis loops, tends to increase as the substrate temperature increases – a trend which was

also seen by Mathet et al. for thicker Pt/Co(1.6nm)/Pt films[18]. The magnetic anisotropy constants K_{eff}, obtained from room-temperature SQUID-VSM measurements with the field applied in the film plane, are larger by a factor of 2-3 than those obtained for Co/Pt multilayers deposited at room temperature (K_{eff} = 127 kJ/m^3) in a previous study[22]. A possible reason for this is that the higher temperatures promote the surface diffusion of Co, leading to longer-range order and increasing the PMA and thus H_c. Hashimoto et al.[23] attributed the origin of the PMA to interfacial effects (interface induced anisotropy) at the Co/Pt boundary and showed that at growth pressures < 4 x 10^{-3} Torr, magnetoelastic effects such as magnetostrictive stress caused by adhesion of the film to the substrate, and a magnetostrictive effect in the strained Co layers, could be neglected. The main pre-requisite for a strong interfacial anisotropy was determined to be the crystallographic continuity of Co, Co-Pt mixture, and Pt layers in the multilayer structure[1,23]. In Figure 3 the PMA does not scale with H_c at the higher substrate temperatures, however, suggesting that at these temperatures the crystallographic continuity may be disturbed, e.g. by Co-Pt intermixing. A similar dependence of PMA on crystal structure was observed in Co_xPt_{1-x} alloys[24].

The coercive fields of the epitaxial layers grown at lower substrate temperature (100°C, 150°C) are similar to those of polycrystalline Co/Pt films grown in an earlier study[25]. Since H_c is controlled by domain nucleation, in order to investigate the DW propagation we measured the DW creep velocity as a function of magnetic field in each epitaxial Co/Pt film. To image magnetic domains, a high resolution wide-field Kerr microscope was used. The film was first saturated out of plane in a field of about +600 Oe. Reverse domains were nucleated by applying a negative field (e.g. -120 Oe), and then expanded by applying additional negative field pulses ranging from 40-800 Oe with durations in the 100 ms range. DW displacements were determined quasi-statically from images of the domain structure

captured in zero field before and after the application of the field pulse. We do not see any difference between the domain pattern that is formed just after the negative field pulse, and the domain pattern while the field is ramped back to zero. The images were subtracted one from the other to give dark contrast in the area swept out by the DW during the field pulse (see Figure 4(a) for an example). The DW velocity was determined from the gradient of a linear fit to the displacement plotted as a function of the pulse duration. In this way, effects from the transient parts of the pulses were eliminated.

Considering the DW as an elastic interface, in the presence of weak disorder the DW is pinned for all driving forces, f, below the depinning force, f_{dep}, at which a critical depinning transition occurs[26]. At finite temperature the depinning transition is smeared due to thermal activation and a finite velocity is expected for all nonzero forces. This is true even for f << f_{dep}, where the thermally activated interface motion is known as creep. In the creep regime the following velocity-field relationship is predicted (H << H_{dep}):

$$v = v_0 \exp\left[-\left(\frac{U_c}{kT}\right)\left(\frac{H_{dep}}{H}\right)^{\mu}\right] \quad (1)$$

Here, U_c is related to the height of the disorder-induced pinning energy barrier, k is the Boltzmann constant, T is the ambient temperature (290 K), H_{dep} is the depinning field, μ is a universal dynamic exponent equal to 1/4 for a 1D interface moving in a 2D weakly disordered medium, and v_0 is a numerical prefactor.

To verify that our DW motion obeys the creep law, we plot ln(*v*) versus $H^{-1/4}$ (Figure 4(b)). Linear behavior is observed at low fields for all films, demonstrating that creep occurs and that μ = ¼. Linear fits to ln(*v*) versus $H^{-1/4}$ give the pinning energies U_c, and these are plotted

as a function of substrate temperature in Figure 4(c). There is a striking correspondence between the behaviors of H_c and U_c as a function of substrate temperature, depicted in Figures 3 and 4(c), respectively. It should be noted that H_{dep} used in the calculation of U_c is not the coercive field but the highest field value that was used in the DW creep measurements (at which flow motion started to appear), and thus, while H_c is determined by domain nucleation, U_c is a reliable indicator of the DW pinning in the films. In the domain images we observe a faster DW creep motion in films grown on the colder substrates (100-150°C), and a larger rate of nucleation for films grown on the hotter substrates (>150°C), which corresponds to the behaviors of H_c and U_c as a function of substrate temperature. Together with the information from the TEM investigation, we thus deduce that the lower substrate temperatures of 100-150°C permit the growth of highly ordered, epitaxial material, with sharp Co/Pt interfaces and few domain wall pinning sites.

The pinning energies may be compared with those measured in polycrystalline Co/Pt[7] using the ratio U_c/kT. We obtain a lowest value of $U_c/kT = 37$ for the film grown at 150°C and a highest value of $U_c/kT = 67$ for the film grown at 250°C. In Ref. [7], it is shown that U_c/kT increases when the thickness of the Co layer is increased, up to a value of 72 for a 1 nm polycrystalline Co layer (obtained by extrapolation of the data). Our epitaxial films contain two 0.5 nm Co layers and all of our U_c/kT values are <72. Furthermore, the DW creep velocities obtained in our experiments (~300 μm/s at ~200 Oe in the film grown at 150°C) are approximately 2-3 times higher than the velocities obtained in polycrystalline Co/Pt[6]. This suggests that there is an improvement in DW creep velocity in very highly ordered epitaxial films.

In summary, the magnetic properties of epitaxial Co/Pt may be tuned by choosing an appropriate substrate temperature during sputter-deposition. Maintaining the C-plane sapphire substrate at a temperature in the range 450-550°C ensures the Pt seed layer has good (111) texture. When the subsequent Co/Pt layers are sputter-grown at 150°C, a high quality epitaxial film is obtained, as shown by X-ray diffraction and TEM. The coercive field and the effective PMA of the Co/Pt films both increase as the substrate temperature is varied from 100-250°C, with a deviation in scaling at the higher substrate temperatures which may originate from a weakening of the crystallographic order. The moderate DW pinning and high quality epitaxy of the films grown at 100-150°C may prove useful for further studies of DW motion or spin torque.

Acknowledgements

This work was supported by EPSRC (grant numbers EP/I011668/1, EP/I013520/1, EP/K003127/1, EP/G005176/1).

References

[a)]Author to whom correspondence should be addressed. Electronic mail: t.a.moore@leeds.ac.uk

[1] P.F. Carcia, *J. Appl. Phys.* **63**, 5066 (1988)

[2] C.-J. Lin, G.L. Gorman, C.H. Lee, R.F.C. Farrow, E.E. Marinero, H.V. Do, H. Notarys and C.J. Chien, *J. Magn. Magn. Mater.* **93**, 194 (1991)

[3] M. Hartmann, B. A. J. Jacobs and J. J. M. Braat, *Philips Techn. Rev.* **42**, 37 (1985)

[4] W.B. Zeper, F.J.A.M. Greidanus, P.F. Carcia and C.R. Fincher, *J. Appl. Phys.* **65** 4971 (1989)

[5] M. Bauer, A. Mougin, J.P. Jamet, V. Repain, J. Ferré, R.L. Stamps, H. Bernas and C. Chappert, *Phys. Rev. Lett.* **94**, 207211 (2005)

[6] F. Cayssol, D. Ravelosona, C. Chappert, J. Ferré and J.P. Jamet, *Phys. Rev. Lett.* **92**, 107202 (2004)

[7] P.J. Metaxas, J.P. Jamet, A. Mougin, M. Cormier, J. Ferré, V. Baltz, B. Rodmacq, B. Dieny and R.L. Stamps, *Phys. Rev. Lett.* **99**, 217208 (2007)

[8] M.S. Pierce, J.E. Davies, J.J. Turner, K. Chesnel, E.E. Fullerton, J. Nam, R. Hailstone, S.D. Kevan, J.B. Kortright, K. Liu, et al., *Phys. Rev. B* **87**, 184428 (2013)

[9] L. San Emeterio Alvarez, K.-Y. Wang, S. Lepadatu, S. Landi, S.J. Bending and C.H. Marrows, *Phys. Rev. Lett.* **104**, 137205 (2010)

[10] M. Cormier, A. Mougin, J. Ferré, A. Thiaville, N. Charpentier, F. Piéchon, R. Weil, V. Baltz and B. Rodmacq, *Phys. Rev. B* **81**, 024407 (2010)

[11] K.-J. Kim, J.-C. Lee, S.-J. Yun, G.-H. Gim, K.-S. Lee, S.-B. Choe and K.-H. Shin, *Appl. Phys. Express* **3**, 083001 (2010)

[12] I.M. Miron, T. Moore, H. Szambolics, L.D. Buda-Prejbeanu, S. Auffret, B. Rodmacq, S. Pizzini, J. Vogel, M. Bonfim, A. Schuhl, et al., *Nat. Mater.* **10**, 419 (2011)

[13] L. Liu, O.J. Lee, T.J. Gudmundsen, D.C. Ralph and R.A. Buhrman, *Phys. Rev. Lett.* **109**, 096602 (2012)

[14] S.S.P. Parkin, M. Hayashi and L. Thomas, *Science* **190**, 320 (2008)

[15] B.D. Hermsmeier, R.F.C. Farrow, C.H. Lee, E.E. Marinero, C.J. Lin, R.F. Marks and C.J. Chien, *J. Appl. Phys.* **69**, 5646 (1991)

[16] P.F. Carcia, Z.G. Li and W.B. Zeper, *J. Magn. Magn. Mater.* **121**, 452 (1993)

[17] C.L. Canedy, X.W. Li and G. Xiao, *J. Appl. Phys.* **81**, 5367 (1997)

[18] V. Mathet, T. Devolder, C. Chappert, J. Ferré, S. Lemerle, L. Belliard and G. Guentherodt, *J. Magn. Magn. Mater.* **260**, 295 (2003)

[19] M. Björck and G. Andersson, *J. Appl. Cryst.* **40**, 1174 (2007)

[20] M. Björck, *J. Appl. Cryst.* **44**, 1198 (2011)

[21] C. Kooy and U. Enz, *Philips Res. Rep.* **15**, 7 (1960)

[22] S. Landis, B. Rodmacq and B. Dieny, *Phys. Rev. B* **62**, 12271 (2000)

[23] S. Hashimoto, Y. Ochiai and K. Aso, *J. Appl. Phys.* **66**, 4909 (1989)

[24] M. Maret, M.C. Cadeville, W. Staiger, E. Beaurepaire, R. Poinsot and A. Herr, *Thin Solid Films* **275**, 224 (1996)

[25] K. Wang, M.-C. Wu, S. Lepadatu, J.S. Claydon, C.H. Marrows and S.J. Bending, *J. Appl. Phys.* **110**, 083913 (2011)

[26] P. Chauve, T. Giamarchi and P. Le Doussal, *Phys. Rev. B* **62**, 6241 (2000)

Figure captions

Figure 1. X-ray diffraction spectra for a single 60 nm Pt film and for Pt(3.0nm)/[Co(t)/Pt(1.0nm)]$_{10}$, where t = 0.5, 1.0, 1.3 nm. The 60 nm and 3.0 nm Pt layers were deposited at a substrate temperature of 450°C, while the [Co/Pt] layers were deposited at 80°C.

Figure 2. (a) HAADF STEM image of Pt(3.0nm)/Co(0.7nm)/Pt(1.0nm), where the upper Co/Pt layers were deposited at 150°C. A scan was performed over an area of 6x6 nm^2 whose position is indicated by the square. The profile from the scan is depicted in (b).

Figure 3. Coercivity H_c (filled squares) and effective perpendicular anisotropy constant K_{eff} (open circles) of Pt(3.0nm)/[Co(0.5nm)/Pt(1.0nm)]$_2$. The upper Co/Pt layers were deposited at substrate temperatures in the range 100-250°C.

Figure 4. (a) Wide-field Kerr microscope image of a DW displacement. The black region denotes the area covered by the DW during the field pulse. Displacements were measured at three locations (d1, d2, d3) on each image, averaged, and plotted as a function of pulse duration to obtain the DW velocity. (b) Natural logarithm of DW velocity, ln(v), as a function of applied field H raised to the power -1/4, for Pt(3.0nm)/[Co(0.5nm)/Pt(1.0nm)]$_2$ with the upper Co/Pt layers deposited at various substrate temperatures. (c) Pinning energy U_c as a function of the substrate temperature during growth of the Co/Pt.

Figure 1

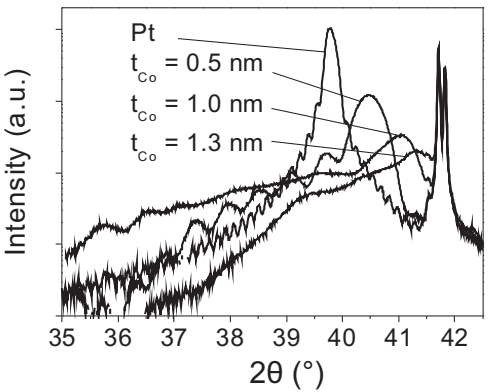
Pt
t_{Co} = 0.5 nm
t_{Co} = 1.0 nm
t_{Co} = 1.3 nm
Intensity (a.u.)
35
36
37
38
39
40
41
42
2θ (°)

Figure 2

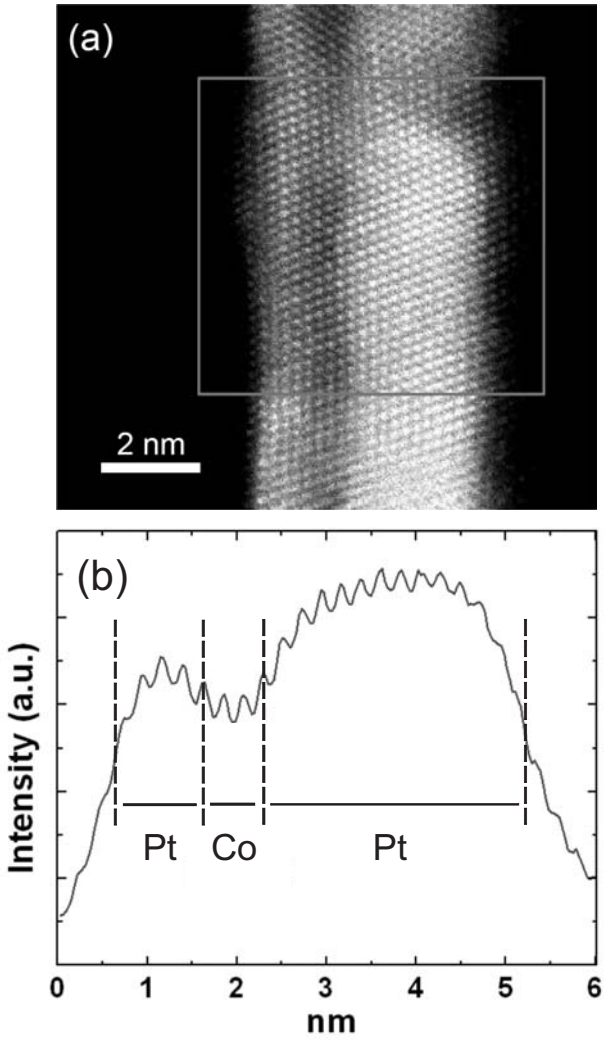

Figure 3

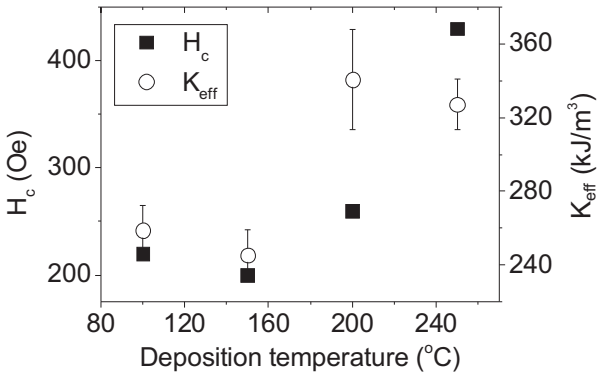
H_c
K_eff
400
300
200
360
320
280
240
80
120
160
200
240
H_c (Oe)
K_eff (kJ/m^3)
Deposition temperature (°C)

Figure 4

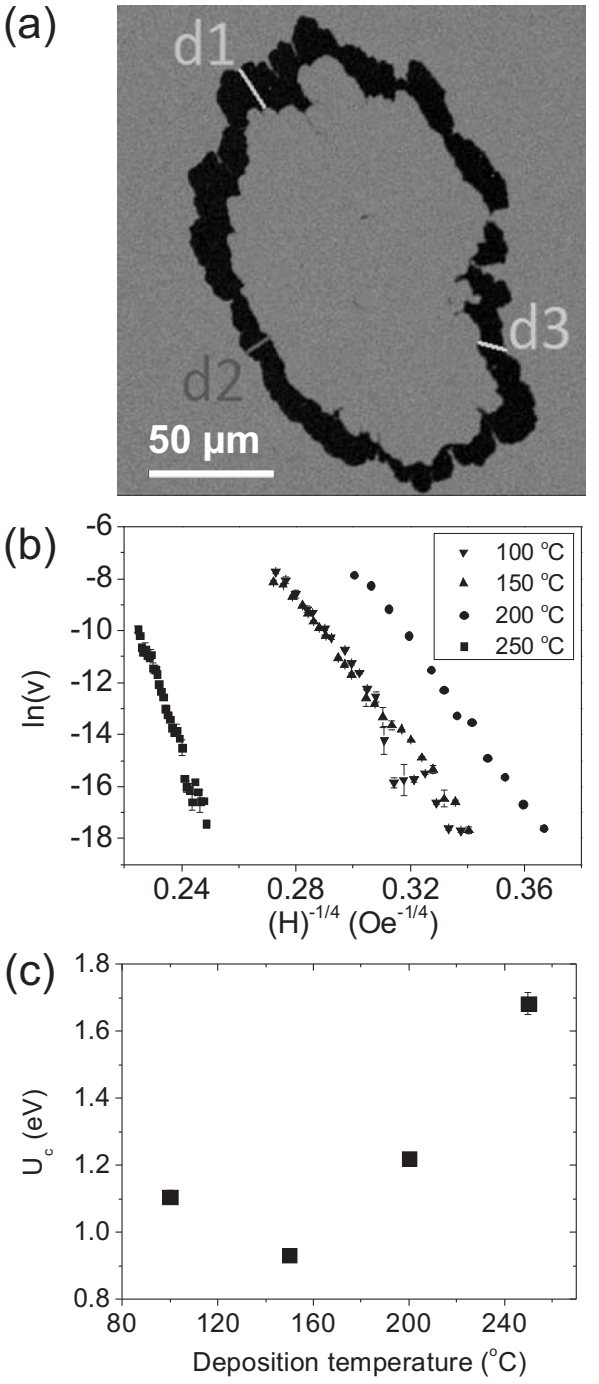
(a)
d1
d2
d3
50 μm
(b)
100 ℃
150 ℃
200 ℃
250 ℃
ln(v)
-6
-8
-10
-12
-14
-16
-18
0.24
0.28
0.32
0.36
(H)^-1/4 (Oe^-1/4)
(c)
U_c (eV)
1.8
1.6
1.4
1.2
1.0
0.8
80
120
160
200
240
Deposition temperature (°C)